Radiation Measurements 99 (2017) 10–17

Contents lists available at ScienceDirect

Radiation Measurements

journal homepage: www.elsevier.com/locate/radmeas

Thermoluminescence associated with two-electron traps

R. Chen [a, *], J.L. Lawless [b], V. Pagonis [c]

[a] Raymond and Beverly Sackler School of Physics and Astronomy, Tel Aviv University, Tel Aviv 69978, Israel
[b] Redwood Scientific Incorporated, Pacifica, CA 94044-4300, USA
[c] Physics Department, McDaniel College, Westminster, MD 21157, USA

HIGHLIGHTS

- A TL model based on a two-electron trap and one center is presented.
- Numerical simulation and approximate analytical results are given.
- A glow curve with two peaks is deduced.
- An effect of very strong superlinearity, with cubic dose dependence is explained.

ARTICLE INFO

Article history:
Received 20 January 2017
Received in revised form
6 March 2017
Accepted 6 March 2017
Available online 9 March 2017

ABSTRACT

A model of thermoluminescence (TL) is presented based on a double-occupancy electron trap and a single-hole recombination center. The concept of double-electron traps has been established before with regard to different solid state phenomena and briefly mentioned as a possible occurrence in connection with TL. A new set of simultaneous differential equations governing the three stages of excitation, relaxation and readout of TL in this new framework is developed. This situation is dealt with by solving these sets of equations sequentially for reasonable sets of chosen trapping parameters. Also, an analytical treatment using plausible simplifying assumptions is given in parallel. The outcome of these procedures yields a two-peak TL curve and, in a sense, the two-electron trap behaves as two traps with different activation energies, frequency factors and retrapping probabilities. The results of the simulations and the approximate analytical approach show that the lower-temperature peak has features of first-order peak and is strongly superlinear with the dose of excitation. With the appropriate choice of parameters, the dose dependence of the first peak has been found to be cubic and slightly more than cubic with the excitation dose. This may explain experimental results of cubic and somewhat stronger superlinearity previously reported in the literature. The second peak has second-order features and it shifts dramatically to lower temperatures with increasing dose.

1. Introduction

May and Partridge (1964) tried to explain the results of thermoluminescence (TL) in KCl, which exhibited an approximate non-integer order of kinetics of ~1.5 by assuming an electron trap with two electrons. They suggested that two electrons may be located in a single lattice site or in two sites with very close proximity. The activation process would consist of excitation of both electrons simultaneously into the activated state. By using some simplifying assumption, they reached a 1.5-order equation for TL.

The concept of two-electron traps has been mentioned in the literature for the explanation of different solid-state phenomena. Jaros (1975) dealt with the photo-ionization spectra of GaP:O and suggested that the impurity potential is strong enough to bind a second electron. Jaros has performed a convergent calculation of the two-electron state associated with O in GaP. Kaufmann and Schneider (1977) have shown by ESR measurements that neutral substitutional iron impurities in GaP can trap two electrons. Mircea et al. (1977) considered the occurrence of two-electron traps in the explanation of the results of transient-capacity-spectroscopy in $Ga_{1-x}In_xAs$ with $0 < x < 0.21$. Lee and Crawford (1977) discussed the two-electron center in Al_2O_3 and Summers et al. (1983) communicated on two-electron vacancies in MgO. Kaufmann et al. (1979) reported on infrared luminescence and EPR in GaP:Ni and

* Corresponding author.
E-mail address: chenr@tau.ac.il (R. Chen).

http://dx.doi.org/10.1016/j.radmeas.2017.03.002
1350-4487/

explained the results by asserting that the Ni^+ is a two-electron trap state. Matsuda and Ohata (1981, 1982) described a model of a two-electron capture process with a typical example of GaP:O. Binbin and Chihtang (2011) considered the trapping capacitance of 2-charge-state impurities in Metal-Oxide-Semiconductor Capacitors (MOSC's). They mentioned impurities in Si such as a two-electron trap associated with Sulfur and a two-hole trap ascribed to Zinc impurity. A number of papers reported on effects associated with two-electron traps in alkalihalides. Nahum (1967) described the luminescence of different centers in LiF and mentioned the effect of two-electron capture. Porret and Lüty (1971) reported on luminescence of F centers in KCl, and described the formation of a two-electron F′ center. Baldacchini et al. (1981) communicated on radiative and nonradiative processes of F and F′ centers in NaBr and NaI, concentrating on the role of two-electronic states. Zhang et al. (1994) also discussed the two-electron systems in ionic crystals, and in particular, the role of F′ centers in alkalihalides. The two-electron F′ centers in alkalihalides have been broadly discussed by Georgiev (1988).

A rather similar situation of two-hole centers has been considered in the literature. Winter et al. (1969) reported on the dichroism of V bands in potassium and rubidium halides and explained the results using a model of two holes trapped at an anion in a cation vacancy. More specifically, with regard to TL, Mayhugh (1970) and Townsend et al. (1979) explained results of thermoluminescence in LiF by the existence of V_3 centers containing two trapped holes. Böhm and Scharmann (1981) mentioned the two-electron F′ center in alkalihalides with relation to the general subject of TL dosimetry. Yazici et al. (2004) who studied TL of LiF:Mg, Ti between 100 and 300 K suggested that their results are related to the V_3 two-hole centers. The same V_3 two-hole centers have been considered as being associated with TL by Horowitz (2006) and by Eliyahu et al. (2016). Woda and Wagner (2007), in an explanation of a non-monotonic dose dependence of Ge- and Ti-centers in quartz, discuss a model of double-electron capture which can be expressed in both ESR and TL measurements.

It is worth mentioning that the distinction between traps and centers is in their role during the read-out stage. For the sake of simplicity, we usually talk about electron traps and hole centers, but the inverse situation is just as likely to occur. The real distinction should be made between the active and passive entities. Traps are active in the sense that they release thermally or optically carriers into the conduction or valence bands or into an excited state within the forbidden gap. In the former case, the free electrons or holes can move in their respective bands before encountering stationary holes or electron in a center and recombination takes place yielding energy that may or may not be luminescence photons. In the latter case of a carrier being elevated into an excited state within the forbidden gap, recombination takes place within the same locality where the trap and center are.

The same is true for two-electron and two-hole entities. It is convenient to speak about a two-electron trap as the entity which can release thermally or optically sequentially two electrons into the conduction band before their recombination with a stationary hole and about two-hole centers which can recombine sequentially with two free electrons from the conduction band. However, here too, the mirror image situation is feasible all the same. We will continue to talk about the two-electron trap and two-hole luminescence centers, but will keep in mind that the inverse situation is possible. The sets of simultaneous differential equations governing the processes for these two sets of circumstances are exactly the same.

In the present paper we concentrate on a model of two-charge-carrier traps whereas the subject of two-carrier centers and their relation to TL will be discussed elsewhere.

2. The model

At present, we consider a model of two-electron traps in the study of thermoluminescence. As opposed to the work by May and Partridge (1964) we assume that the two electrons are thermally stimulated not simultaneously into the conduction band and that the activation energies as well as the other trapping parameters of the two electrons are not the same. The model is similar to that given previously by Woda and Wagner (2007) except that the authors deal mainly with ESR measurements and therefore, limit their study to the excitation stage whereas here we talk about TL and take into consideration the three stages of TL, namely, excitation, relaxation and heating. Also, these authors concentrate on the non-monotonic dose dependence of trap filling whereas we deal with properties of the TL curve resulting from this model, and in particular the superlinear dose dependence.

Let us assume a simple system with one trap and one center. However, let us assume that the trap can capture two electrons. A schematic energy-level diagram of the model is shown in Fig. 1. Let us denote the total concentration of traps by N (cm^{-3}). Out of these, it may have instantaneously n_1 (cm^{-3}) traps with single electrons or n_2 (cm^{-3}) traps with two electrons. Obviously, the instantaneous concentration of empty traps is $N\text{-}n_1\text{-}n_2$. The activation energy of a single electron in a trap will be denoted by E_1 (eV) and the energy for releasing an electron from a trap with two electrons is denoted by E_2 (eV). It seems reasonable to assume that $E_1 > E_2$ since, with two electrons in a trap, there may be Coulombic repulsion and, with one electron, there may be some Coulombic attraction of the free electron to the impurity ion forming the trap. The trapping probability coefficients will be denoted by A_1 and A_2, where A_1 (cm^3s^{-1}) is the trapping probability coefficient into an empty trap and A_2 (cm^3s^{-1}) the trapping probability coefficient into a trap with one electron. It appears that usually, $A_1 > A_2$ since the probability to capture a free electron is expected to be larger in an empty trap than in a trap with one electron. The frequency factors for the first and second electron are s_1 (s^{-1}) and s_2 (s^{-1}), respectively. They may not necessarily be the same since the thermal release of the first and second electrons are not from exactly the same environment. m (cm^{-3}) denotes the instantaneous concentration of holes in centers out of a total of M (cm^{-3}) centers. n_c (cm^{-3}) is the instantaneous concentration of free electrons and A_m (cm^3s^{-1}) the recombination-probability coefficient. In the excitation stage, X ($cm^{-3}s^{-1}$) denotes the rate of production of electron-hole pairs, which is proportional to the dose rate of excitation. Note that if we denote the time of excitation by t_D (s), then $D = X \cdot t_D$ (cm^{-3}) is the total concentration

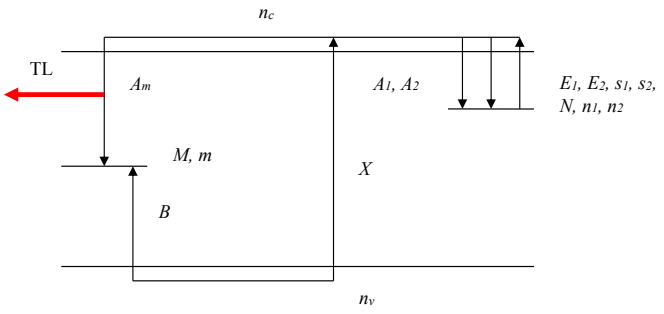

Fig. 1. Energy level diagram of a solid with a single-hole center and a two-electron trap. The transitions during excitation and heating are shown. The meaning of the different parameters and functions are given in the text.

of pairs produced by the irradiation, which is proportional to the total applied dose. n_v (cm^{-3}) denotes the instantaneous concentration of free holes and B (cm^3s^{-1}) is the probability coefficient of capturing free holes in the recombination center.

Under these circumstances, the set of coupled differential equations governing the process during excitation would be:

$$\frac{dm}{dt} = Bn_v(M-m) - A_m m n_c, \tag{1}$$

$$\frac{dn_1}{dt} = s_2 n_2 \exp(-E_2/kT) + A_1(N-n_1-n_2)n_c - s_1 n_1 \exp(-E_1/kT) - A_2 n_1 n_c, \tag{2}$$

$$\frac{dn_2}{dt} = A_2 n_1 n_c - s_2 n_2 \exp(-E_2/kT), \tag{3}$$

$$n_c + n_1 + 2n_2 = m + n_v, \tag{4}$$

$$\frac{dn_v}{dt} = X - Bn_v(M-m). \tag{5}$$

It should be mentioned that Eq. (4) can be written in a differential form, namely,

$$\frac{dn_c}{dt} = \frac{dm}{dt} + \frac{dn_v}{dt} - \frac{dn_1}{dt} - 2\frac{dn_2}{dt}. \tag{4a}$$

Note the first term on the right-hand side of Eq. (3). It has to do with the retrapping of an electron from the conduction band with a trap with one electron, changing it to be a trap with two electrons. Note also the factor 2 in the charge balance Eq. (4). Since n_2 is the concentration of traps with two electrons, the total instantaneous concentration of electrons in these traps is $2n_2$. The same factor of 2 appears also in Eq. (4a). These equations are practically the same as those given by Woda and Wagner with regard to the trap filling measured by ESR. It is worth mentioning that as long as the temperature during excitation is significantly lower than that of the TL peaks, the exponential terms in Eqs. (2) and (3) may be negligibly small.

In order to follow the experimental procedure, we add following the excitation stage a relaxation stage which mimics the time between excitation and heating. We use the values of the concentrations at the end of excitation as initial values for the relaxation stage, set $X = 0$, and solve the simultaneous equations for a further period of time until n_c and n_v are practically zero.

The same equations can be used for the heating stage by keeping $X = 0$ and letting the temperature in Eqs. (2) and (3) to increase according to the heating function. We have used, as is customary, a linear heating function with a heating rate of 1 Ks^{-1}. Like before, we use the final concentrations of the relaxation period as initial values for the heating stage. According to this model, the concentration of free holes n_v during the heating stage is nil. Here, Eq. (1) is replaced by

$$I = -\frac{dm}{dt} = A_m m n_c, \tag{6}$$

where I is the intensity of the emitted TL light. Also, since in this stage, $n_v \equiv 0$, we have $dn_v/dt \equiv 0$ and Eq. (5) can be disregarded. Thus, in order to follow the process for the heating stage, we solve numerically the simultaneous Eqs (2) (3) (4a) and (6). Note that, as given here, I has units of $cm^{-3}s^{-1}$. In fact, a dimensional constant should have been inserted here, which is arbitrarily set to unity.

3. Numerical results

The following parameters have been used for the excitation, relaxation and heating: $B = 10^{-13}$ cm^3s^{-1}; $A_m = 10^{-11}$ cm^3s^{-1}; $A_1 = 10^{-12}$ cm^3s^{-1}; $A_2 = 10^{-14}$ cm^3s^{-1}; $s_1 = 10^{12}$ s^{-1}; $s_2 = 10^{13}$ s^{-1}; $E_1 = 1.3$ eV; $E_2 = 0.7$ eV; $N = 10^{17}$ cm^{-3}; $M = 10^{16}$ cm^{-3}.

Fig. 2 depicts the results of the simulation by solving numerically the mentioned set of differential equations in the sequence of excitation, relaxation and heating. The dose rate X used in Fig. 2 was 1.024×10^{14} cm^3s^{-1} and the time of excitation was $t_D = 100$ s. The temperature of excitation was 200 K. However, when we repeated the simulation with excitation at 300 K, the second peak came out exactly the same. The intensities of the simulated two peaks have been found to be significantly different and in order to be able to see both of them on the same scale, intensities below 350 K were multiplied by a factor of 1000. In further simulations, the dose rates X chosen varied from 2.5×10^{10} to 1.024×10^{14} cm^3s^{-1} by factors of 2. The first peak, occurring at ~250 K has been found to have a symmetry factor $\mu_g = 0.421$ characteristic of first-order kinetics. Evaluating the activation energy using the standard shape formula (Chen, 1969) yielded $E = 0.697$ eV as compared to the inserted value of $E_2 = 0.7$ eV. The frequency factor was found to be $s = 8.4 \times 10^{12}$ s^{-1} as compared to the value used for simulation, $s_2 = 10^{13}s^{-1}$. Peak #2 yielded $\mu_g = 0.49$, indicating second order. The calculated activation energy is E = 1.32 eV as compared to the input of $E_1 = 1.3$ eV and the evaluated frequency factor is $s = 8 \times 10^{11}$ s^{-1} as compared to the inserted $s_1 = 10^{12}$ s^{-1}. The agreement between inserted and evaluated parameters is very good. Typically for first-order peaks, the maximum temperature of the first peak does not vary with the dose. The second peak looks like a second-order peak and as such, its maximum temperature varies significantly with the dose. From the lowest dose used of 2.5×10^{12} cm^{-3} to the highest one of 1.024×10^{16} cm^{-3}, the temperature moved from 663 K down to 508 K.

An interesting feature has been found in the dose dependence of the first peak; it depended on the dose in a strong superlinear manner. In the simulations, the dose-rate X has been varied between 2.5×10^{10} and 1.024×0^{14} $cm^{-3}s^{-1}$ by a factor of 2 in the dose rate between consecutive simulations, and with the given value of t_D, the dose has thus been between 2.5×10^{12} and

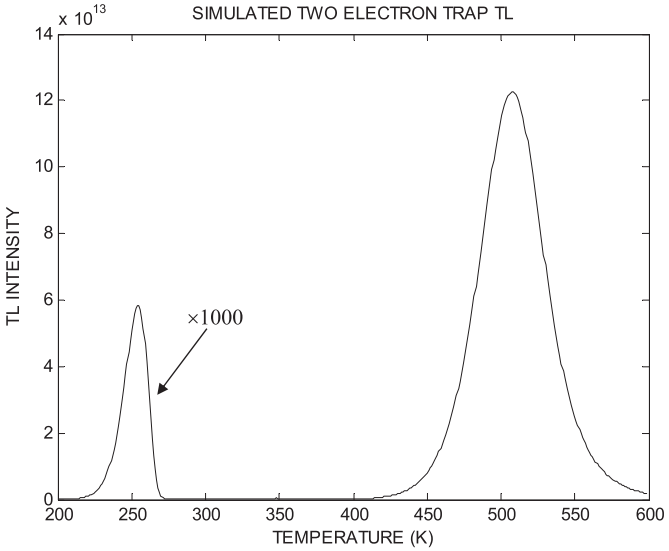

Fig. 2. Simulated glow curve from a two-electron trap model. The set of parameters is given in the text.

1.024×10^{16} cm^{-3}. Note, however that exactly the same results were reached when the dose rate was kept constant at 2.5×10^{10} cm^{-3}s^{-1} and the time of excitation changed gradually from 100 to 8.192×10^{5} s. The results of dose dependence of the area under the first TL peak are shown in curve (a) of Fig. 3 on a log-log scale. The initial slope on this scale is three, indicating a cubic dependence on the dose. At higher doses, the slope gets smaller but is still larger than unity indicating superlinearity. Since the shape of this peak does not change with the applied dose, it is obvious that the area under the curve increases in the same strong superlinear manner.

It should be noted that an initial cubic dose dependence of TL has been reported in the literature for at least three cases of TL dose dependence. Halperin and Chen (1966) described the results of UV excited TL in semiconducting diamonds. When the excitation was by UV light in the range of 300–400 nm, the initial dose dependence was $\propto D^3$. Chen et al. (1988) communicated on the dose dependence of TL in β-irradiated synthetic quartz. They found cubic dose dependence in beta excited samples prior to any initial heating. Otaki et al. (1994) reported on more than cubic dose dependence in UV excited CaF_2:Tb_4O_7.

As for the second peak in the simulations, the dose dependence of its maximum is very slightly superlinear. As pointed out by Chen et al. (1983), the initial dose dependence of the maximum of a second-order peak is $\sim D^{1.07}$, and this is also the case here. Note that, in fact, in this case, the area under the TL peak is linear with the dose as is seen in curve (b) of Fig. 3 and the slight superlinearity of the maximum intensity is ascribed to a small change in the shape of the curve. As the dose grows, the peak gets somewhat narrower and since the area under the curve remains constant, the maximum intensity grows a little faster than linearly. At the high-dose range, some saturation effect comes into play and the increase of I_m gets somewhat sublinear.

In order to distinguish between processes taking place during excitation and heating, we have plotted the concentrations $n_{1,0}$, $n_{2,0}$ and m_0 at the end of the relaxation stage and prior to the heating as simulated with the mentioned set of parameters. The results are shown in Fig. 4 on a log-log scale in the range of doses between 3×10^{11} and 10^{16} cm^{-3}. Note that the figure shows both the numerical results of the simulations and the analytical results discussed below. As is seen in the figure, $n_{1,0}$ and m_0 grow linearly with the dose and have practically the same values up to the point that the occupancy in the center m reaches the full capacity of

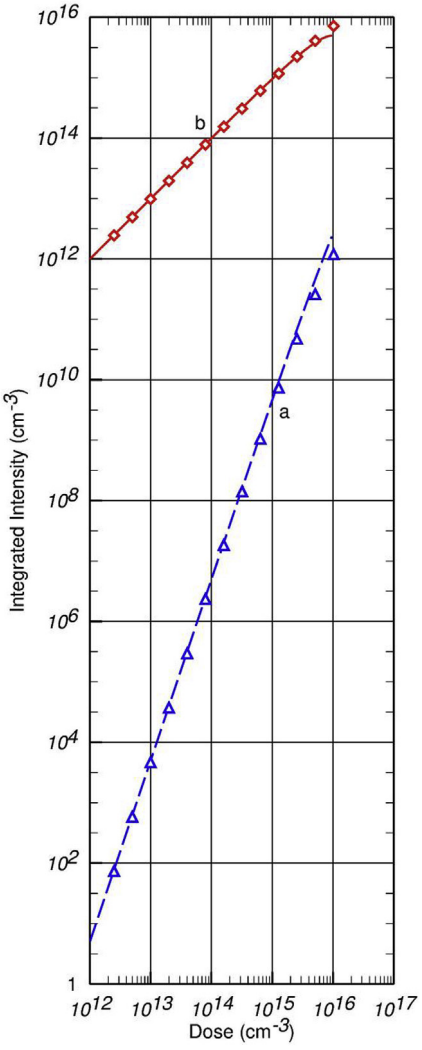

Fig. 3. Dependence of the area under the two simulated TL peaks on dose of excitation plotted on a log-log scale, (a) the lower temperature peak; the dashed line shows the results of Eq. (44) and the triangles represent the numerical results. (b) the higher temperature peak; the solid line shows the results from Eq. (28) and the diamonds are the numerical results.

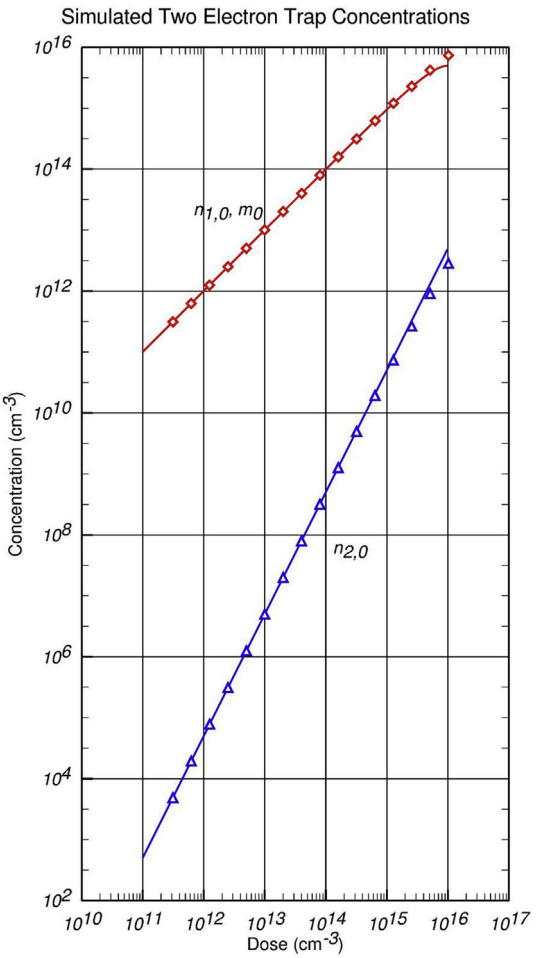

Fig. 4. The dependence of the simulated trap and center occupancies at the end of excitation and relaxation on the dose of excitation on a log-log scale. The solid lines indicate the results from Eqs. (26–28). The diamonds show the numerical results of n_1 and m from the numerical simulations and the triangles are the numerical results of n_2.

$M = 10^{16}$ cm^{-3}. It is worth mentioning that, at least for the given set of parameters, we have all along $n_{1,0} \cong m_0 \cong D$ where D is the "dose" given in the same units of cm^{-3}. As for the curve of $n_{2,0}$, it has a slope of 2 at the lower doses, indicating quadratic dose dependence. At higher doses, the slope reduces to ~1.65 before m_0 goes to saturation.

4. Theoretical background

4.1. The excitation stage

Let us assume that irradiation takes place at low temperature. As pointed out above, the temperature dependent terms in Eqs. (2) and (3) can be neglected so for this stage we can consider Eqs. (1)–(5) without these terms. In addition, the initial conditions are $m(0) = n_1(0) = n_2(0) = 0$. Let us assume that the time of excitation t_D is long enough so that

$$1 << B(M-m)t_D, \tag{7}$$

$$1 << [A_1(N-n_1-n_2) + A_2 n_1 + A_m m]t_D. \tag{8}$$

In other words, we assume that the lifetimes of free electrons and free holes are much shorter than the irradiation time. Since irradiation typically takes place over seconds, days or years and the lifetimes are often measured in microseconds, this is generally a good approximation. From Eqs. (4) and (5) we get respectively

$$n_c = \frac{X}{A_1(N-n_1-n_2) + A_2 n_1 + A_m m}, \tag{9}$$

$$n_v = \frac{X}{B(M-m)}. \tag{10}$$

In Eqs. (9) and (10), the numerator represents the production rate of free electrons and holes and the denominators represent constants for their capture.

The governing equations then reduce to

$$\frac{dn_1}{dt} = \frac{A_1(N-n_1-n_2) - A_2 n_1}{A_1(N-n_1-n_2) + A_2 n_1 + A_m m} X, \tag{11}$$

$$\frac{dn_2}{dt} = \frac{A_2 n_1}{A_1(N-n_1-n_2) + A_2 n_1 + A_m m} X, \tag{12}$$

$$\frac{dm}{dt} = X - \frac{A_m m}{A_1(N-n_1-n_2) + A_2 n_1 + A_m m} X. \tag{13}$$

Eq. (12) shows that the rate of increase of the population of n_2 is proportional to the rate of production of free electrons, X, multiplied by the fraction of those electrons that are captured by n_1, creating n_2. Eq. (11) similarly shows that the rate of increase of the population n_1 is proportional to the rate of production. The factor in front of X in Eq. (11) represents the fraction of those free electrons that are captured into n_1 minus the fraction that converts n_1 to n_2. Eq. (13) shows that the rate of increase of the population of holes, m, is the rate of free hole production, X, minus the rate of free electron production, X, times the fraction of those free electrons that end up recombining in the center.

Eq. (11) through (13) can be combined to again yield conservation of charge

$$m = n_1 + 2n_2, \tag{14}$$

where we used the initial condition $m(0) = n_1(0) = n_2(0) = 0$. Note that Eq. (14) may result from Eq. (4) by assuming that n_v and n_c are negligibly small as compared to the other magnitudes, which is usually made in the quasi-equilibrium assumptions.

4.2. Complete irradiation solution for a special case

If the rate constants have a given relative size, we can obtain a solution that is valid all the way from low doses to high doses. In particular, let us consider

$$A_m = A_2 = A_1/2. \tag{15}$$

Note that we are not assuming any particular values for the rate constants but only require that their relative sizes be given by Eq. (15). Eqs. (11) and (12) simplify to

$$\frac{dn_1}{dt} = \frac{2N - 3n_1 - 2n_2}{2N} X, \tag{16}$$

$$\frac{dn_2}{dt} = \frac{n_1}{2N} X, \tag{17}$$

where Eq. (14) was used. By the usual methods and using the initial conditions $m(0) = n_1(0) = n_2(0) = 0$, the solution is found to be

$$n_1 = 2N\left[\exp\left(-\frac{Xt}{2N}\right) - \exp\left(-\frac{Xt}{N}\right)\right], \tag{18}$$

$$n_2 = N\left[1 - 2\exp\left(-\frac{Xt}{2N}\right) + \exp\left(-\frac{Xt}{N}\right)\right], \tag{19}$$

$$m = n_1 + 2n_2 = 2N\left[1 - \exp\left(-\frac{Xt}{2N}\right)\right]. \tag{20}$$

From these equations, one can see that there are two time constants that govern the growth of the populations of n_1 and n_2. Note that, as long as Eq. (15) holds, we can raise or lower the rate constants A_1, A_2 and A_m, and it has no effect on these time constants.

The concentrations of n_1, n_2 and m vs. dose are shown in Fig. 5.

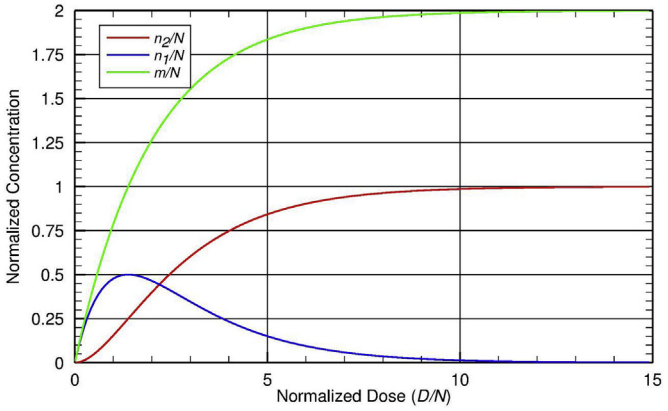

Fig. 5. Trap concentrations plotted against the dose for the case $A_m = A_2 = A_1/2$. The theory also assumes that $M > 2N$ and that A_1 is large enough so that the quasi-steady theory holds. Subject to these requirements, this is a universal plot: whatever values one picks for X, t, A_1, N, the solution falls on this plot.

We can see that at low doses, n_1 and m rise linearly with dose. Consequently, n_2 rises superlinearly with the dose. Eventually, as dose increases, the conversion of n_1 to n_2 occurs faster than n_1 is formed. The population of n_1 reaches a peak and then declines. With high enough dose, all the electron traps are converted to n_2 as the population of n_1 asymptotically approaches zero. Because n_2 is the concentration of two-electron occupied traps, the population of m asymptotically approaches $2N$. This figure bears similarity to Fig. 7 in the paper by Woda and Wagner (2007) except that with the parameters they chose only very slight superlinearity was found there for n_2. Note also that their results are found by numerical simulations whereas ours in Fig. 5 result from approximate analytical considerations.

4.3. Irradiation solution for small doses

Let us assume that the dose is low enough so that the concentrations are well below saturation. In particular, we assume that the dose is small enough so that

$$(A_1 + A_2 + A_m)n_1 << A_1 N, \tag{21}$$

$$(A_1 + 2A_m)n_2 << A_1 N. \tag{22}$$

With this assumption, the governing equations can be expanded in a Taylor series in powers of (n_1/N) and (n_2/N),

$$\frac{dn_1}{dt} = \left(1 - \frac{A_m + 2A_2}{A_1}\frac{n_1}{N} - \frac{2A_m}{A_1}\frac{n_2}{N} + \ldots\right)X, \tag{23}$$

$$\frac{dn_2}{dt} = \left(0 + \frac{A_2 n_1}{A_1 N} + \ldots\right)X, \tag{24}$$

$$\frac{dm}{dt} = \left(1 - \frac{A_m m}{A_1 N} + \ldots\right)X. \tag{25}$$

With the dose D defined as $D = \int X dt$, the above integrates to

$$n_1 = D - \frac{A_m + 2A_2}{A_1 N_1}\frac{D^2}{2} + O\left(D^3\right), \tag{26}$$

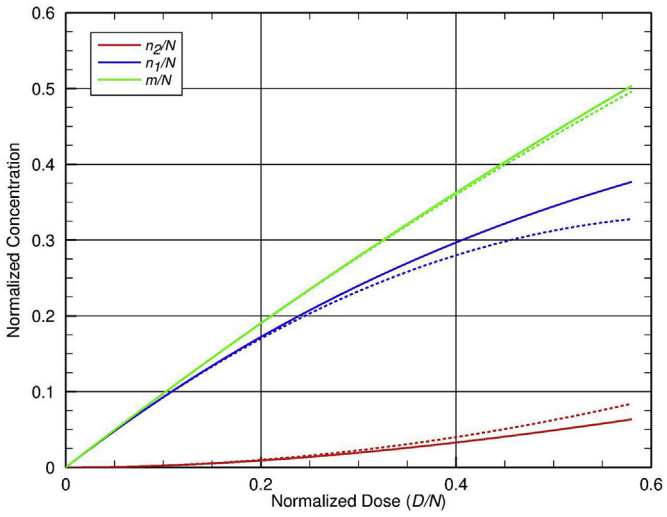

Fig. 6. Trap concentrations at low doses. The solid curves are the results of the theory for $A_m = A_2 = A_1/2$. The dotted curves are the low-dose approximation.

$$n_2 = \frac{A_2}{A_1 N}\frac{D^2}{2} + O\left(D^3\right), \tag{27}$$

$$m = D - \frac{A_m}{A_1 N}\frac{D^2}{2} + O\left(D^3\right). \tag{28}$$

This shows that, at least at small doses, both n_1 and m are linear in dose while n_2 rises quadratically with dose, in agreement with the numerical results shown in Fig. 4 above. The low-dose approximation is compared to the full analytical solution of Eqs. (18) and (19) in Fig. 6. This low-dose approximation appears reasonably accurate up to doses of $D \approx 0.4N$.

5. The heating stage

5.1. The governing equations

We will examine the equations for heating during the time over which luminescence due to recombination of electrons released by thermal excitation from n_2 is important. We find that the competition between trapping into n_1 and recombination leads to superlinearity at low doses. When we combine the heating theory with the irradiation theory, a cubic superlinearity is found.

The set of simultaneous differential equations governing the heating stage is rather similar to Eqs. (1)–(5) governing the excitation stage, but with the appropriate adjustments. During heating, $n_v \equiv 0$ and therefore Eq. (5) is superfluous. Also, obviously, $X \equiv 0$ and also, the temperature is variable, $T = T_0 + \beta t$ where T_0 (K) is the initial temperature, and β (K/s) the constant heating rate. The governing equations are

$$\frac{dn_1}{dt} = A_1(N - n_1 - n_2)n_c - A_2 n_1 n_c + n_2 s_2 \exp(-E_2/kT) - n_1 s_1 \exp(-E_1/kT), \tag{29}$$

$$\frac{dn_2}{dt} - A_2 n_1 n_c - n_2 s_2 \exp(-E_2/kT), \tag{30}$$

$$\frac{dm}{dt} = -A_m m n_c, \tag{31}$$

$$\frac{dn_c}{dt} = -A_1(N - n_1 - n_2)n_c - A_2 n_1 n_c - A_m m n_c + n_1 s_1 \exp(-E_1/kT) + n_2 s_2 \exp(-E_2/kT). \tag{32}$$

In the heating stage, we have $n_v \equiv 0$, and therefore, using the conventional quasi-equilibrium assumption,

$$n_c << n_1, n_2, m, \tag{33}$$

Eq. (4) reads

$$m = n_1 + 2n_2, \tag{34}$$

or in its differential form,

$$\frac{dm}{dt} = \frac{dn_1}{dt} + 2\frac{dn_2}{dt}. \tag{35}$$

Inserting Eqs. (29–31) into Eq. (35) and rearranging, one gets

$$n_c = \frac{n_1 s_1 \exp(E_1/kT) + n_2 s_2 \exp(E_2/kT)}{A_1(N - n_1 - n_2) + A_2 n_1 + A_m m}. \tag{36}$$

The governing equations now reduce to

$$\frac{dn_1}{dt} = \frac{[2A_1(N-n_1-n_2)+A_m m]n_2 s_2 \exp(-E_2/kT) - (2A_2 n_1 + A_m m)n_1 s_1 \exp(-E_1/kT)}{A_1(N-n_1-n_2)+A_2 n_1 + A_m m}, \quad (37)$$

$$\frac{dn_2}{dt} = \frac{A_2 n_1 s_1 \exp(-E_1/kT) - [A_1(N-n_1-n_2)+A_m m]n_2 s_2 \exp(-E_2/kT)}{A_1(N-n_1-n_2)+A_2 n_1 + A_m m}, \quad (38)$$

$$\frac{dm}{dt} = -\frac{A_m m[n_1 s_1 \exp(-E_1/kT) + n_2 s_2 \exp(-E_2/kT)]}{A_1(N-n_1-n_2)+A_2 n_1 + A_m m}. \quad (39)$$

As pointed out above, since the charge of n_2 is more negative than that of n_1, we expect that $E_2 < E_1$. Consistent with that (and as seen in the results of the simulations in Fig. 2), let us assume that the thermal excitation of an electron from a double-charged trap effectively completes before significant thermal excitation from the single-charged trap begins. In this case, we neglect $n_1 s_1 \exp(-E_1/kT)$ relative to $n_2 s_2 \exp(-E_2/kT)$. Eqs. (38) and (39) can now be combined to yield

$$\frac{dm}{dt} = \frac{A_m m}{A_1(N-n_1-n_2)+A_m m}\frac{dn_2}{dt}. \quad (40)$$

This equation will be useful in the next section.

5.2. Approximation for small n_2

Let us assume further that $n_2 << n_1$. This will always be true at low doses and will also be true at higher doses if A_2 is smaller than A_1 as is usually expected given the charge difference. From $n_2 << n_1$, it also follows that $n_2 << m$ and $n_1 \approx m$. Eq. (40) further simplifies now to

$$\frac{dm}{dt} = \frac{A_m m}{A_1 N + (A_m - A_1)m}\frac{dn_2}{dt}. \quad (41)$$

Because $n_2 << m$, it follows that there will be a small reduction in m to

$$m = m_0 - \frac{A_m m_0}{A_1 N + (A_m - A_1)m_0} n_{2,0}, \quad (42)$$

where the subscript 0 indicates values at the start of heating. It follows from Eq. (42) that the integrated intensity during the thermal depletion of the double-charged trap is

$$I_2 = \frac{A_m m_0}{A_1 N + (A_m - A_1)m_0} n_{2,0}. \quad (43)$$

Because both m_0 and $n_{2,0}$ increase with the dose at least linearly at the low-dose range, this indicates a superlinear dependence.

If we further assume low doses so that Eqs. (27, 28) can be applied, we have

$$I_2 = \frac{A_m A_2}{2A_1 N}\frac{D^3}{A_1 N + (A_m - A_1)D}. \quad (44)$$

This shows a cubic dependence on the dose and sometimes even faster, as discussed below.

6. Discussion

In this work, we have presented a new model that can explain a very strongly superlinear dose dependence of thermoluminescence. The model is based on the assumption that a trap that may capture either one or two electrons takes part in the process. As pointed out above, the occurrence of such traps has been proposed in different solid state phenomena including TL. It should be noted that models that lead to superlinear dose dependence have been offered before. These models dealt with competition between two traps, or two centers and distinguished between competition during excitation, during heating or both (see e.g. Kristianpoller et al., 1974; Bowman and Chen, 1979; Chen and Fogel, 1993; Chen et al., 1996). These models could explain a quadratic and to some extent, more than quadratic behavior at least in the low dose range. In the literature, there are, however, at least three examples of cubic dose dependence. Halperin and Chen (1966) reported on cubic dose dependence of UV excited TL in semiconducting diamonds, Chen et al. (1988) described a similar effect of TL in β-excited quartz and Otaki et al. (1994) communicated on more than cubic dose dependence in CaF_2:Tb_4O_7.

In the present case, the occurrence of traps that may hold either one or two electrons explains cubic dose dependence as is seen in Eq. (44). In a sense, it seems that there is competition between the two states of the trap, namely, if it holds a single or double electron. As can be seen both in the simulations and the approximate analytical treatment, after irradiation + relaxation, the concentration of n_2 scales as dose squared. This seems to be due to competition between trapping of an electron in an empty trap, $A_1(N-n_1-n_2)n_c$ and trapping in a trap with one electron, $A_2 n_1 n_c$. During readout, there is competition between trapping in an empty trap, $A_1(N-n_1-n_2)n_c$ and recombination, $A_m m n_c$. With m increasing with dose, this adds an additional linear term which makes the total dependence of the first peak cubic.

If $A_m >> A_1$ (as is the case in the simulations above), Eq. (44) predicts a fall off from the cubic dependence as doses approach $D \sim (A_1/A_m)N$. If the low-dose approximation still applies above this dose, then the dose dependence will be quadratic. Note that Eq. (44) implies faster-than-cubic superlinearity if $A_m < A_1$. This is so since in Eq. (44), if the dose D increases, the denominator decreases, which causes the whole expression to increase somewhat faster than D^3. As pointed out, this agrees with the results by Otaki et al. (1994).

As mentioned above, under the given circumstances, $E_1 > E_2$, and therefore, $T_{m1} > T_{m2}$, namely, the peak associated with two trapped electrons occurs before the peak ascribed to only one trapped electron. As indicated above, the first peak is asymmetric, with a shape factor of a first-order peak. The second peak is nearly symmetric, as is characteristic of second-order peaks. This is in agreement with the known property of a series of peaks as

described by Chen and Pagonis (2013); the peaks excluding the last in a series tend to be of first order and the last one tends to have second-order symmetry. As is characteristic of first-order peaks here, the maximum temperature of the first peak which grows strongly superlinearly does not change with the excitation dose. As for the second peak, it shifts very significantly to lower temperatures; such shift to lower temperature is characteristic of second-order peaks, but the amount of the shift here is rather large. Note that such significant shift has been reported by Sunta (2015, p. 78) for "regular" simulated second-order TL peak when the excitation dose varies by ~5 orders of magnitude. The parameters retrieved from the simulated peaks using the peak-shape method are very close to those used in the simulation.

References

Baldacchini, G., Pan, D.S., Lüty, F., 1981. Radiative and nonradiative processes of F and F' centers in NaBr and NaI. Phys. Rev. B24, 2174–2186.

Binbin, J., Chihtang, S., 2011. MOS capacitance-Voltage characteristics. III. Trapping capacitance from 2-charge-state impurities. J. Semicond. 32 (121002), 1–16.

Böhm, M., Scharmann, A., 1981. In: Oberhofer, M., Scharmann, A. (Eds.), Theory, Applied Thermoluminescence Dosimetry, Ch. 2, pp. 11–38.

Bowman, S.G.E., Chen, R., 1979. Superlinear filling of traps in crystals due to competition during heating. J. Lumin 18/19, 345–348.

Chen, R., 1969. On the calculation of activation energies and frequency factors from glow curves. J. Appl. Phys. 40, 570–585.

Chen, R., Huntley, J.R., Berger, G.W., 1983. Analysis of TL data dominated by second-order kinetics. Phys. Stat. Sol. (a) 79, 251–261.

Chen, R., Yang, X.H., McKeever, S.W.S., 1988. The strongly superlinear dose dependence of thermoluminescence in synthetic quartz. J. Phys. D. Appl. Phys. 21, 1452–1457.

Chen, R., Fogel, G., 1993. Superlinearity in thermoluminescence revisited. Radiat. Prot. Dosim. 47, 23–26.

Chen, R., Fogel, G., Lee, C.K., 1996. A new look at the models of the superlinear dose dependence of thermoluminescence. Radiat. Prot. Dosim. 65, 63–68.

Chen, R., Pagonis, V., 2013. On the expected order of kinetics in a series of thermoluminescence (TL) and thermally stimulated conductivity (TSC) peaks. Nucl. Inst. Meth. Phys. Res. B312, 60–69.

Eliyahu, I., Druzhyna, S., Horowitz, Y., Reshes, G., Biderman, S., Oster, L., 2016. Kinetic simulation of charge transfer following 5.08 eV (F band) optical excitation of irradiated LiF: Mg,Ti (TLD-100): participation of holes released via V_3-V_k transformation. Radiat. Meas. 90, 27–32.

Georgiev, M., 1988. F'Centers in Alkali Halides. Springer, Berlin.

Halperin, A., Chen, R., 1966. Thermoluminescence of semiconducting diamonds. Phys. Rev. 148, 839–845.

Horowitz, Y., 2006. A unified and comprehensive theory of the TL dose response of thermoluminescent systems applied to LiF: Mg,Ti. In: Horowitz, Y. (Ed.), Microdosimetric Response of Physical and Biological Systems to Low- and High-LET Radiations. Elsevier, Amsterdam, 75–202.

Jaros, M., 1975. Two-electron impurity states of GaP:O. J. Phys. C. Sol. St. Phys. 8, 2455–2462.

Kaufmann, U., Schneider, J., 1977. ESR identification of the iron double electron trap state in GaP. Sol. St. Comm. 21, 1073–1075.

Kaufmann, U., Koschell, W.H., Schneider, J., Weber, J., 1979. Optical and EPR study of the nickel two-electron-trap state in GaP. Phys. Rev. B19, 3343–3352.

Kristianpoller, N., Chen, R., Israeli, M., 1974. Dose dependence of thermoluminescence peaks. J. Phys. D. Appl. Phys. 7, 1063–1072.

Lee, K.H., Crawford Jr., J.H., 1977. Electron centers in single crystal Al_2O_3. Phys. Rev. B15, 4065–4070.

Matsuda, T., Ohata, N., 1981. A simple and exactly soluble model for a deep two-electron trap. Sol. St. Comm. 39, 687–690.

Matsuda, T., Ohata, N., 1982. A simple and exactly soluble model of a deep two-electron trap. II. Sol. St. Comm. 42, 615–618.

May, C.E., Partridge, J.A., 1964. Thermoluminescence kinetics of alpha-irradiated allkali halides. J. Chem. Phys. 40, 1401–1409.

Mayhugh, M.R., 1970. Color centers and the thermoluminescence mechanism in LiF. J. Appl. Phys. 41, 4776–4782.

Mircea, A., Mitonneau, A., Hallais, J., Jaros, M., 1977. Study of the main electron trap in $Ga_{1-x}In_xAs$ alloys. Phys. Rev. B16, 3665–3675.

Nahum, J., 1967. Optical properties and mechanisms of formation of some F-aggregate centers in LiF. Phys. Rev. 158, 814–825.

Otaki, H., Kido, H., Hiratsuka, A., Fukuda, Y., Takeuchi, N., 1994. Estimation of UV radiation dose using CaF_2:Tb_4O_7 as a thermoluminescence dosimeter. J. Mat. Sci. Lett. 13, 1267–1269.

Porret, F., Lüty, F., 1971. Luminescence and F' formation involving spin-polarized F centers in KCl. Phys. Rev. Lett. 26, 843–846.

Summers, G.P., Wilson, T.M., Jeffries, B.T., Tohver, H.T., Chen, Y., Abraham, M.M., 1983. Luminescence from oxygen vacancies in MgO crystals thermochemically reduced at high temperatures. Phys. Rev. B27, 1283–1291.

Sunta, C.M., 2015. Unraveling Thermoluminescence. Springer, India, New Delhi.

Townsend, P.D., Taylor, G.C., Wintersgill, M.C., 1979. An explanation of the anomalously high activation energies of TL in LiF (TLD 100). Radiat. Eff. 41, 11–16.

Winter, E.M., Wolfe, D.R., Christy, R.W., 1969. Dichroism of V bands in potassium and rubidium halides. Phys. Rev. 186, 949–952.

Woda, C., Wagner, G.A., 2007. Non-monotonic dose dependence of the Ge- and Ti-crnters in quartz. Radiat. Meas. 42, 1441–1452.

Yazici, A.N., Karali, T., Townsend, P.D., Ari, M., 2004. Thermoluminescence studies of LiF: Mg,Ti between 100 and 300K. J. Phys. D. Appl. Phys. 37, 3165–3173.

Zhang, C.G., Leung, C.H., Song, K.S., 1994. Two-electron-defect systems in ionic crystals: applications to F' centres in alkali halides. J. Phys. Condens. Matter 6, 7715–7723.